



## DECREASING METHOD OF RESIDUAL DEFORMATION OF R/C COLUMN AFTER EARTHQUAKE EXCITATION

Mutsumi TANAKA<sup>1</sup>, Fumiya ESAKI<sup>2</sup> and Masayuki ONO<sup>3</sup>

### SUMMARY

In moment resisting R/C frame structures, earthquake energy is absorbed by the hysteresis loop due to the yield of longitudinal reinforcement bars (hereafter referred to as “bars”) in columns or beams. In such structures, the demolition of such structures is inevitable because of their inclination due to the residual lateral drift after severe earthquake excitation even if their collapse is avoided. In order to propose the decreasing method of residual story drift of R/C column after the severe earthquake excitation, twelve 1/3 scale model R/C columns were tested. The experimental results concluded that the residual lateral drift of the column with the unbonded high strength bars scarcely increased.

### INTRODUCTION

R/C structures designed by the ductile type show the flexural failure mode due to the yield of longitudinal reinforcement bars of columns or beams. In such structures, the bond of bars should be secure since earthquake energy is absorbed by the hysteresis loop due to the yield of bars. However, the demolition of such structures is inevitable because of their inclination due to the residual lateral drift after severe earthquake excitation even if their collapse is avoided. The proposition of design method to solve the problem mentioned above can be desired since the performance design of buildings is emphasized in the present day. One of the ways to solve the problem is that the structure with columns whose residual lateral drift scarcely occurs is designed. According to R/C block column tests with the unbonded high strength bars, the lateral shear capacity and the hysteresis energy absorption capacity of columns were low. However, the columns showed the stable hysteresis loop and also their residual lateral drift scarcely occurred ESAKI [1]. The test results gave the hint to propose the column with unbonded high strength bars. However, in the proposed structures with these columns, the story collapse occurs in all probability since the lateral load carrying capacity and energy absorption capacity of the columns are low and consequently the failure of beams is not preceded. These structures need to have the devices whose lateral shear capacity and energy absorption capacity are high. As an example, the proposed structures are

---

<sup>1</sup> Research associate, Dept. of Architecture, Kyushu Kyoritsu University, 1-8 Jiyugaoka Yahatanishi-ku Kitakyushu city Fukuoka 807-8585, Japan. E-mail: mutsumi@kyukyo-u.ac.jp

<sup>2</sup> Professor, Dept. of Architecture, Kyushu Kyoritsu University, Fukuoka, Japan. E-mail: ezaki@kyukyo-u.ac.jp

<sup>3</sup> Professor, Dept. of Architecture, Kinki University, Fukuoka, Japan. E-mail: ono@fuk.kindai.ac.jp

permissible if the multi-story framed shear wall showing the flexural failure mode and the coupling girder or damper to absorb the earthquake energy are used together with the columns.

In order to investigate the hysteresis response of the columns with the unbonded high strength bars, twelve 1/3 scale model R/C columns were tested. The experimental variables were shear span ratio and level of axial stress due to vertical load. In this paper, the effect of the bond and strength of bars on the hysteresis loop was examined by the tests.

## LATERAL LOADING TESTS

### Specimens

Table 1 shows the list of specimens. The specimens are columns that have the normal strength longitudinal bars or the unbonded high strength ones. To make bars unbonded, they were jacketed with vinyl tube. The value of shear-span ratio is 2.0 and 1.5. Axial force ratio is 0.15 or 0.30. The name of specimen is showed by three distinction signs of  $a-b-c$ .  $a$  shows the classification of bars.  $B$  denotes the column with deformed bar.  $UB$  denotes the column with unbonded high strength bar.  $UBT$  denotes the column whose top and bottom regions are jacketed with square steel tube.  $b$  shows shear span ratio.  $c$  shows axial force ratio ( $=N/N_0$ ,  $N$ =axial force,  $N_0=bD\sigma_B$ , where  $b$  is the width of column,  $D$  is the depth of column and  $\sigma_B$  is the compressive strength of concrete cylinder, respectively). The mechanical properties of reinforcement and concrete are shown in Table 2.

**Table 1 List of specimen**

(All dimensions in mm)

Specimen	shear-span ratio 2.0			shear-span ratio 1.5		
	<i>B-2-0.15(0.3)</i>	<i>UB-2-0.15(0.3)</i>	<i>UBT-2-0.15(0.3)</i>	<i>B-1.5-0.15(0.3)</i>	<i>UB-1.5-0.15(0.3)</i>	<i>UBT-1.5-0.15(0.3)</i>
Longitudinal reinforcement	6-D13( $p_g=1.91\%$ )	4-9.2 $\phi$ ( $p_g=0.65\%$ )	4-9.2 $\phi$ ( $p_g=0.65\%$ )	6-D10( $p_g=1.07\%$ )	4-9.2 $\phi$ ( $p_g=0.65\%$ )	4-9.2 $\phi$ ( $p_g=0.65\%$ )
Arrangement of hoops	D6@30( $p_w=1.07\%$ ) D6@40( $p_w=0.80\%$ )					
Steel tube			□ -200×200×2.3			□ -200×200×2.3

Note:  $p_g$  = longitudinal reinforcement ratio ( $=a_g/(bD)$ ),  $a_g$  = cross sectional area of longitudinal reinforcement  
 $p_w$  = transverse reinforcement ratio ( $=a_w/(bx)$ ),  $a_w$  = area of a pair of hoops,  $x$  = spacing of hoops

**Table 2 Mechanical properties of reinforcement and concrete**

(1)reinforcement

	$a(cm^2)$	$\sigma_y(MPa)$	$\sigma_u(MPa)$	$E_s(GPa)$	$\epsilon(\%)$
D6	0.32	429	522	170	19.9
D10	0.71	329	478	176	24.9
D13	1.27	360	502	178	18.9
9.2 $\phi$	0.66	1036	1078	181	11.8
PL2.3	0.28	393	431	201	27.8

$a$  : cross sectional area

$\sigma_y$  : yield strength

$\sigma_u$  : tensile strength

$E_s$  : Young's modulus

$\epsilon$  : elongation

(2)concrete

	$\sigma_B(MPa)$	$\epsilon_B$	$E_C(GPa)$
axial force ratio 0.15	28.4	0.00121	28.1
axial force ratio 0.3	20.8	0.00152	25.9

$\sigma_B$  : compressive strength

$\epsilon_B$  : strain at peak stress

$E_C$  : Young's modulus

### Loading Setup and Program

The loading setup is shown in Fig. 1. The loading pattern was cyclic pattern with alternating drift reversed as shown in Fig. 2. The constant vertical load applied to specimens was maintained during lateral loading test.

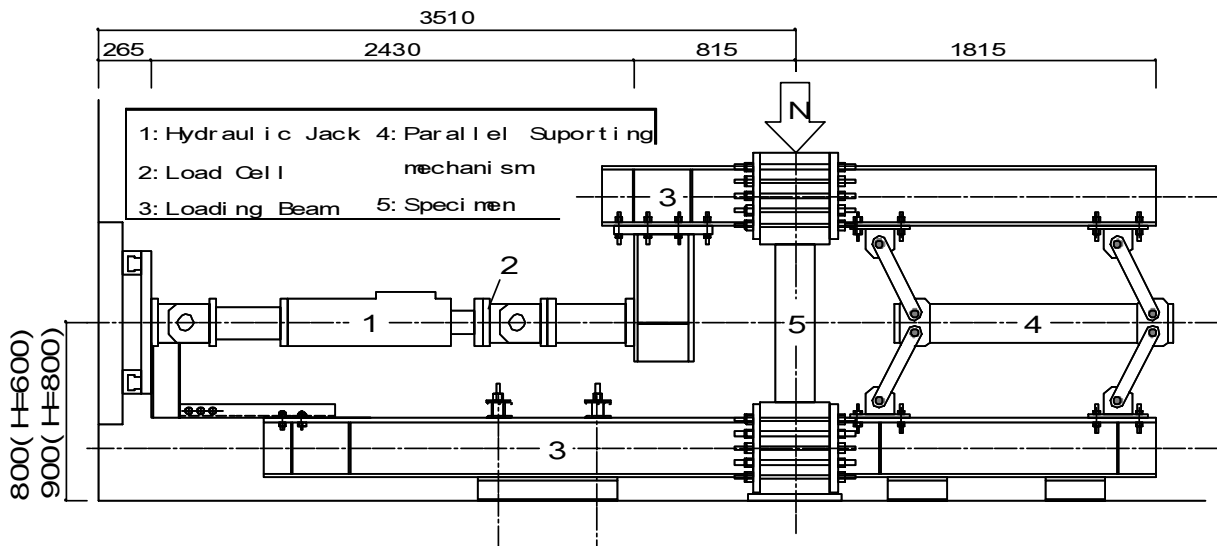


**Fig. 1 Loading setup**

### Measurement System

The lateral and vertical displacements between upper and lower stubs were measured by high sensitive electric transducers (HSETs, 200 $\mu$ /mm and 500 $\mu$ /mm) attached to the measurement system shown in Fig. 3. The strains of longitudinal reinforcement bars and hoops were measured by wire strain gauges pasted at top region, bottom one and other three points divided by four between top and bottom regions. Also, the strains of hoops were measured by wire strain gauges pasted at top, middle and bottom regions.

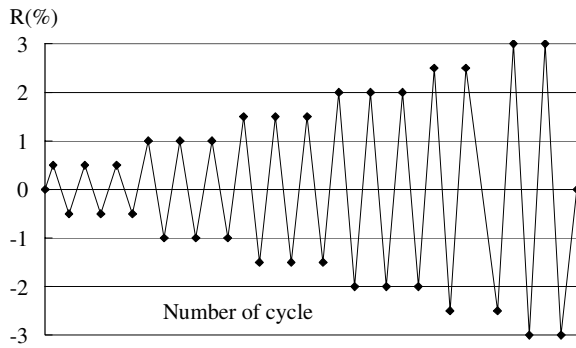


Fig. 2 Loading program

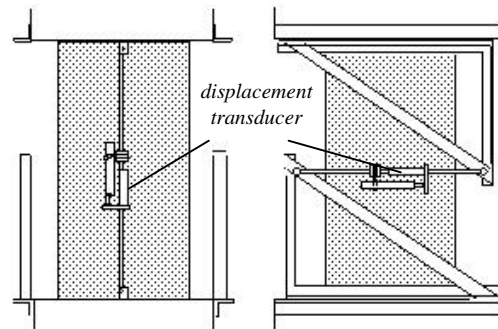


Fig.3 Measurement System

### TEST RESULTS

The strain distribution of bars at  $R=\pm 1\%$  was shown in Fig. 4. The bars nearly yielded and also their bond stress act in the B type specimens. On the other hand, the bars did not yield and also their bond stress did not act in the UB and UBT type specimens.

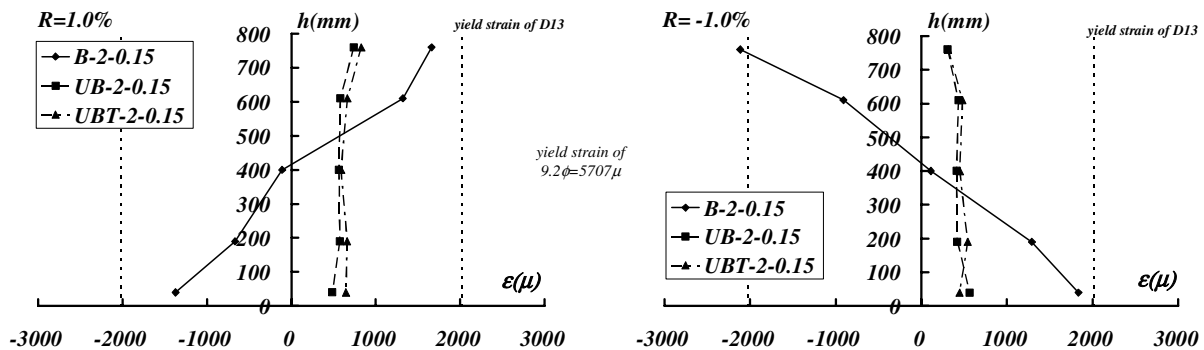


Fig. 4 Strain distribution of bars

The test results are summarized in Table 3. Figure 5 shows lateral load,  $Q$  – drift angle,  $R$ , hysteresis response for shear-span ratio 2 and 1.5 test series specimens, respectively. The drift angle,  $R$ , was obtained by dividing relative lateral displacement between upper and lower stubs by clear height of column. Also, the vertical average strain,  $\epsilon_v$  – drift angle,  $R$ , hysteresis response was shown in Fig. 6.

In the B type specimens, the first flexural crack was observed in the region of  $0.5D$  apart from the end of stub at  $R=0.5\%$ . Many flexural and shear cracks occurred in the region of  $D$  apart from top and bottom ends of column beyond 2% of drift angle. The spalling of cover concrete was observed at ultimate stage. B type specimens showed typical flexural failure mode. The calculated lateral carrying capacity by the equation AIJ [2] was shown with broken line in the figure of  $Q-R$  hysteresis loop. The observed lateral load carrying capacity of the specimens agreed well with the calculated one. The residual lateral drift angle after unloading increased gradually as the experienced lateral drift angle increased.

In the UB type specimens, the first flexural crack was observed in the top and bottom ends at  $R=0.5\%$ . The width of first crack gradually became wide as the lateral drift increased. The slight spalling of cover concrete was observed in the UB type specimens of axial force ratio 0.3 test series at the ultimate stage and consequently the lateral load carrying capacity slightly deteriorated. On the other hand, in the UBT type specimens, no other cracks except the first crack were observed at the ultimate stage. The jacketing square steel tube is effective to confine the concrete since the potential failure regions are the ends of columns in the columns with the unbonded bars. In all specimens with unbonded bars, the lateral stiffness became weak abruptly after the first cracking. However,  $Q$  slightly increased as  $R$  increased in all specimens.  $Q-R$  hysteresis response was stable since the lateral load carrying capacity did not deteriorate. The hysteresis loop indicated that the energy dissipation capacity was poor since the bond between bars and concrete did not exist. In the UB and UBT specimens, the observed lateral load carrying capacity need to be estimated by calculated one dominated by shear failure since the bars did not yield at the ultimate stage. The calculated lateral load carrying capacity based on the arch mechanism theory KATO [3] is plotted in the figure of  $Q-R$  hysteresis loop. The specimens in the axial force ratio 0.15 test series did not reach the calculated capacity. On the other hand, the specimens in the axial force ratio 0.3 test series reached the calculated capacity. However, all specimens did not fail in shear.

**Table3 Summary of test result**

specimen	Experiment				Calculation	
	Maximum lateral load $Q(kN)$		Drift angle at peak load $R(\%)$		$Q_{fu}(kN)$ [2]	$Q_{su}(kN)$ [3]
	+	-	+	-		
B-2-0.15	87.9	-89.0	0.99	-1.50	91.0	-
B-2-0.3	102.5	-100.9	1.49	-2.00	98.5	-
UB-2-0.15	49.5	-48.6	1.99	-1.51	-	70.0
UB-2-0.3	58.1	-52.0	0.99	-1.51	-	51.0
UBT-2-0.15	52.6	-54.1	2.92	-3.01	-	70.0
UBT-2-0.3	62.8	-59.6	0.99	-2.01	-	51.0
B-1.5-0.15	93.7	-91.5	2.32	-1.83	88.5	-
B-1.5-0.3	108.2	-107.9	1.31	-1.34	95.5	-
UB-1.5-0.15	73.3	-70.4	2.48	-2.01	-	92.2
UB-1.5-0.3	73.8	-82.2	0.98	-1.51	-	67.4
UBT-1.5-0.15	84.1	-86.1	3.99	-3.84	-	92.2
UBT-1.5-0.3	81.3	-84.2	3.48	-3.51	-	67.4

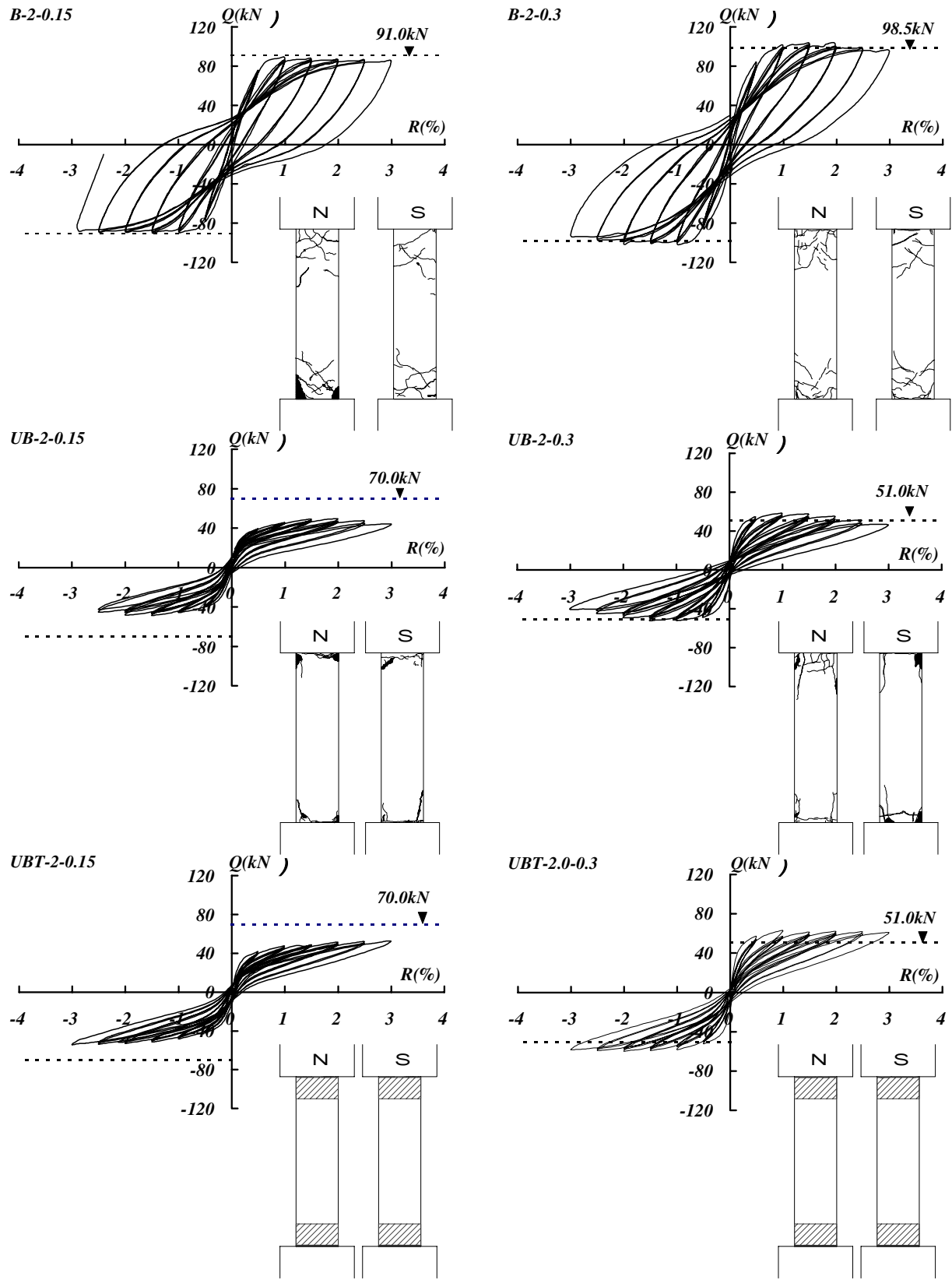


Fig. 5a Lateral load,  $Q$  – drift angle,  $R$ , relationship for shear-span ratio 2 test series specimens

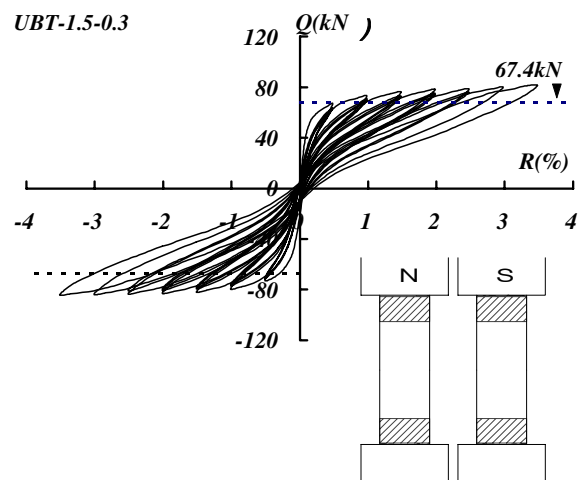
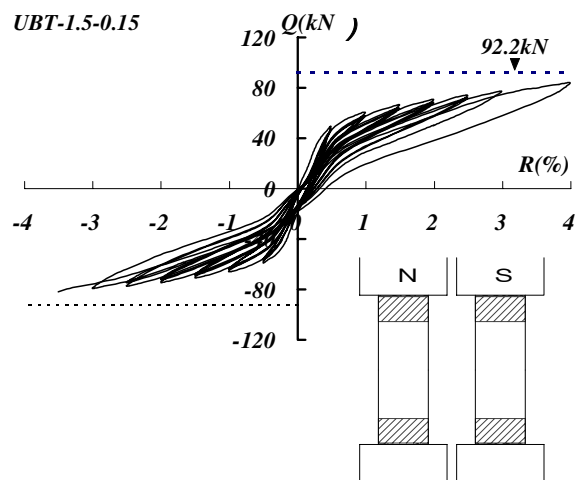
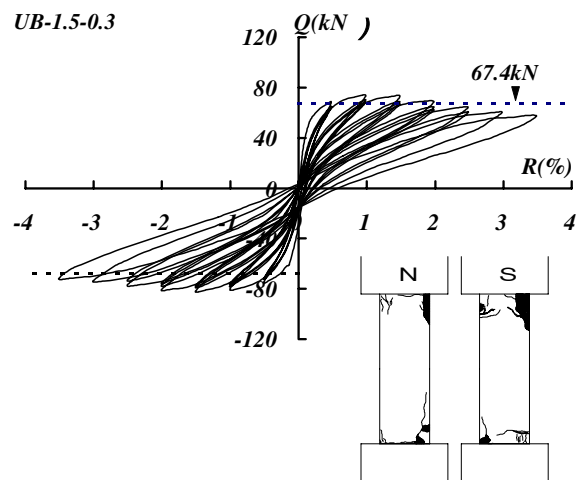
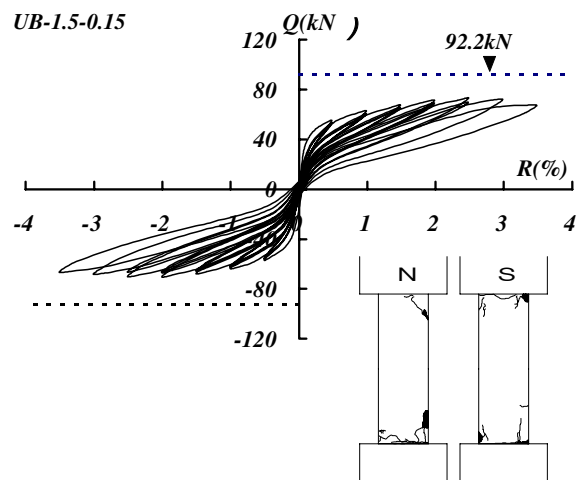
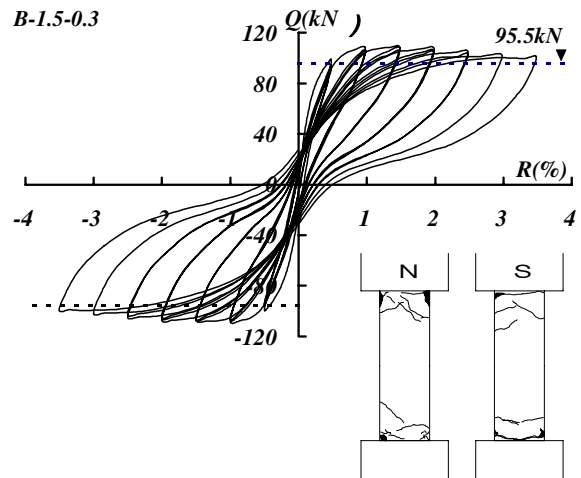
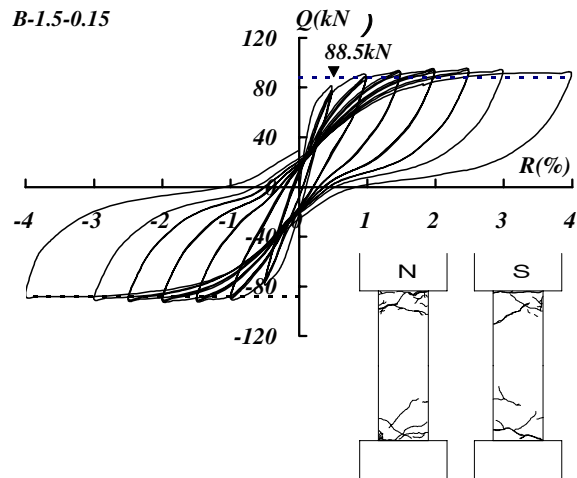


Fig. 5b Lateral load,  $Q$  – drift angle,  $R$ , relationship for shear-span ratio 1.5 test series specimens

Figure 7 shows the relationship between experienced lateral drift angle,  $R_0$ , and residual one after unloading from experienced one,  $R_r$ . In the B type specimens, the residual lateral drift angle increased as the experienced one increased, but in the UB and UBT type specimens, the residual lateral drift angle slightly increased as the experienced one increased.

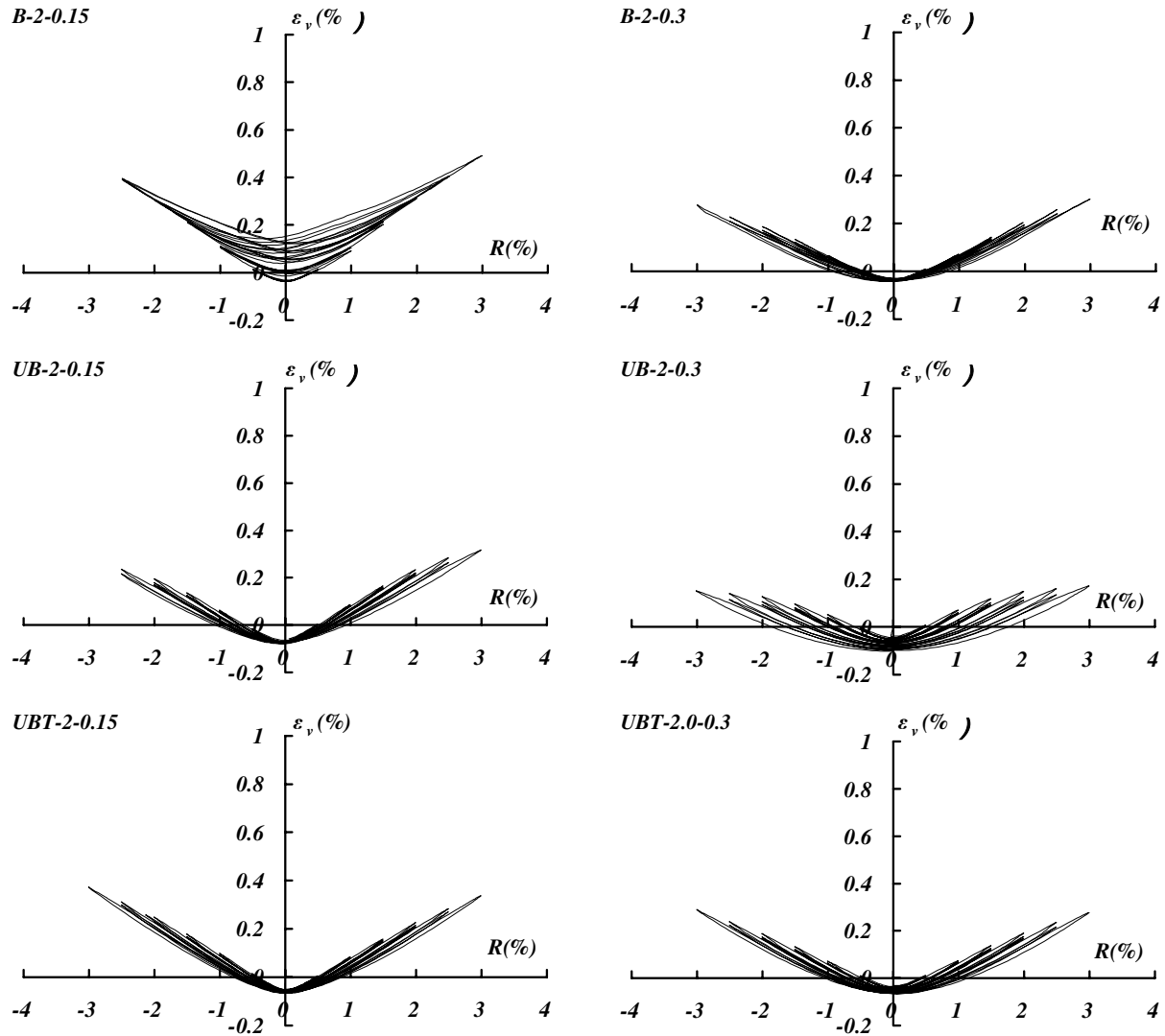
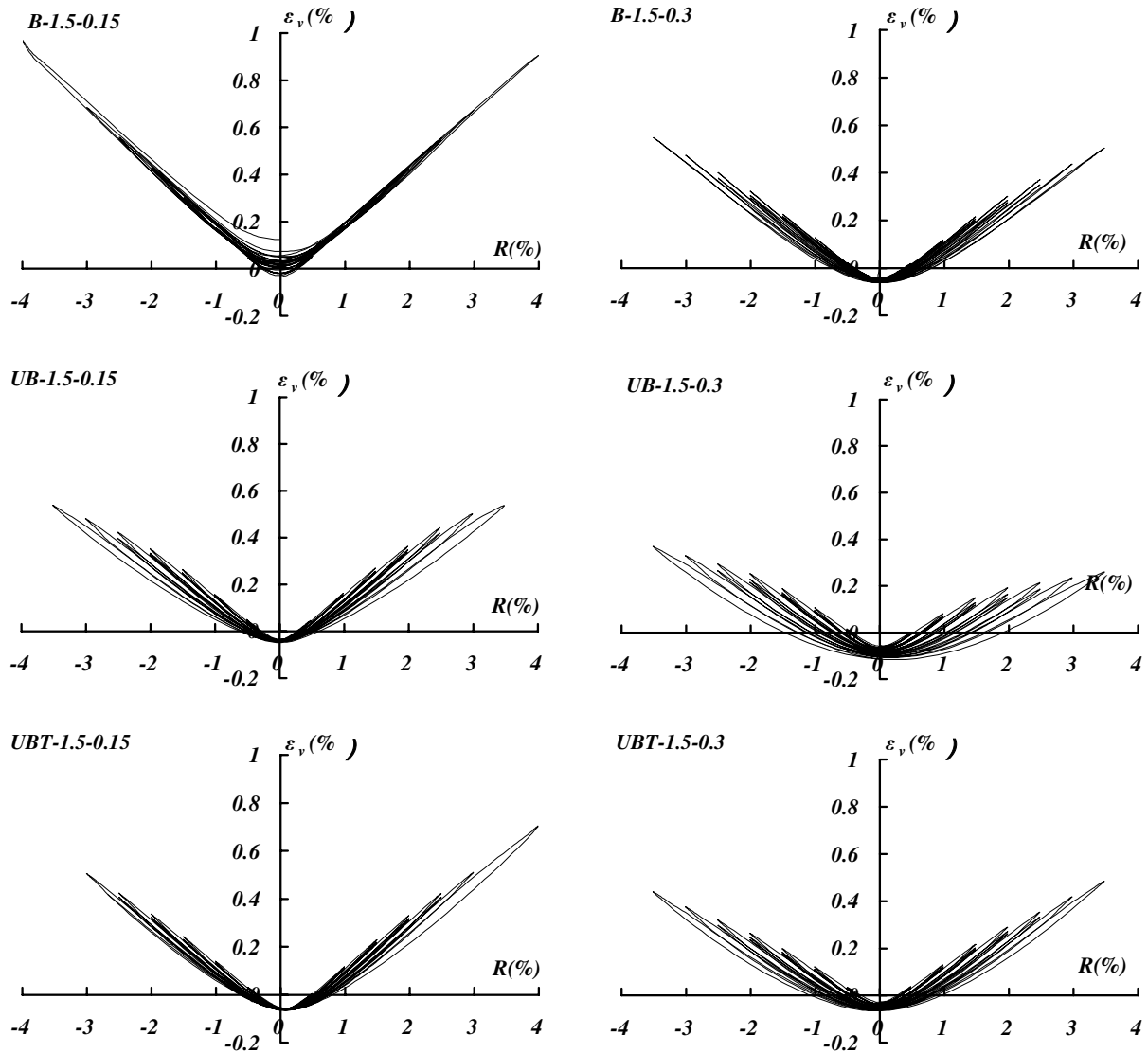


Fig. 6a the vertical average strain,  $\epsilon_v$  – drift angle,  $R$ , relationship for shear-span ratio 2 test series specimens



**Fig. 6b** the vertical average strain,  $\varepsilon_v$  – drift angle,  $R$ , relationship for shear-span ratio 1.5 test series specimens

## CONCLUSIONS

In order to investigate the hysteresis response of columns with the unbonded high strength bars, reversed cyclic lateral loading tests under a constant axial load of columns were conducted. The following conclusions were reached.

- 1) The lateral load carrying capacity of column with unbonded bars is lower than that of column with bonded bars.
- 2) The increase of the residual lateral drift in the columns with unbonded high strength bars was less than that in the columns with bonded normal ones under the large lateral drift.
- 3) If the unbonded high strength longitudinal reinforcement bars are used, the stable hysteresis loop is expected by jacketing the top and bottom ends of column with square steel tube.

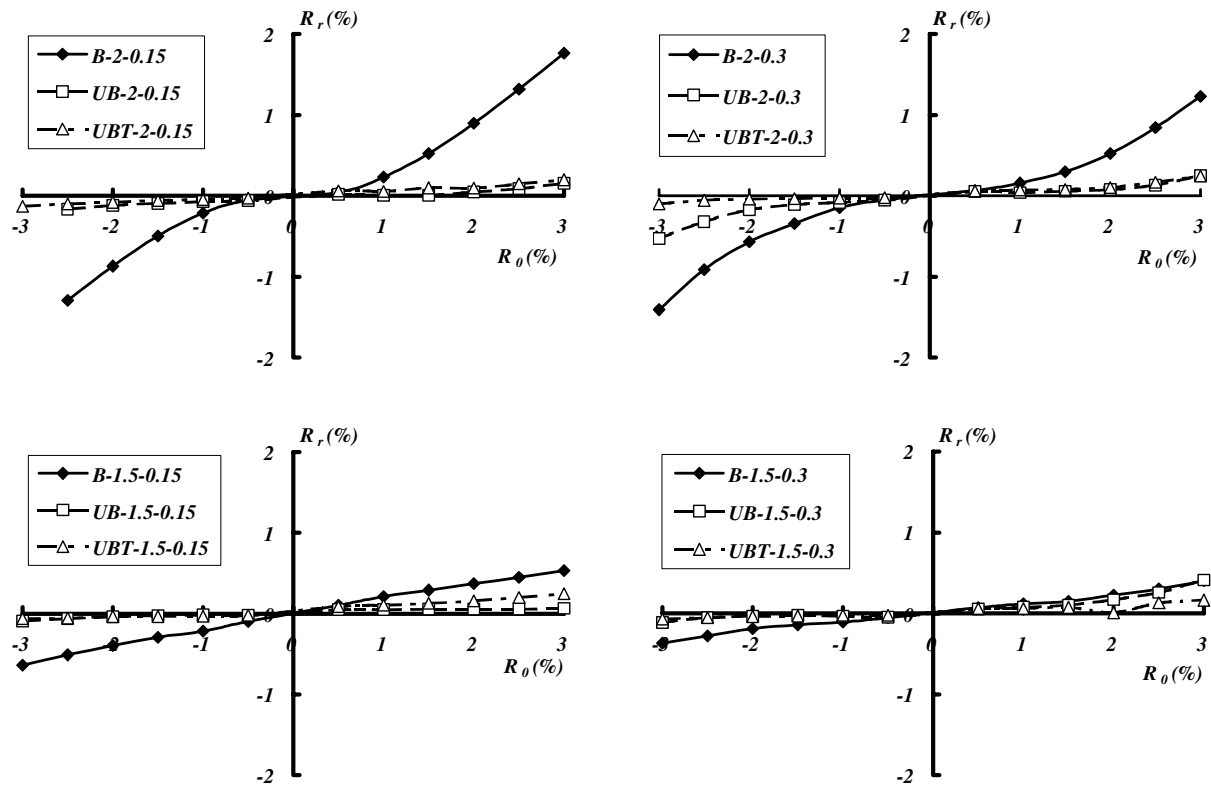


**Fig. 7** The relationship between experienced lateral drift angle,  $R_0$ , and residual one after unloading from experienced one,  $R_r$

#### ACKNOWLEDGMENTS

These experiments were under the Grant in Aid for Scientific Research of the Ministry of Education Culture, Sports, Science and Technology of Japanese Government, assignment No. 15560509. Many students at Kyushu Kyoritsu University (KKU) assisted the experiments. Kazuyoshi TAKADA, Tadamitsu NAGAOKA and Yoshinori YONEHARA who are the technicians at KKU assisted the setup and specimens.

The author would like to thank all the people mentioned for their contribution of this study.

#### REFERENCES

1. Fumiya ESAKI. "Elasto-Plastic Behavior of Recyclable R/C Columns." Proceedings of the Japan Concrete Institute Vol. 20, No. 3: 655-660.
2. Architectural Institute of Japan (1991). "Standard for Structural Calculation of Reinforced Concrete Structures."
3. Ben KATO, Ryoichi SHOHARA. "Strength of steel-reinforced concrete members." Transactions of the Architectural Institute of Japan No, 266 April 1978: 19-29.